SF2A 2006
D. Barret, F. Casoli, T. Contini, G. Lagache, A. Lecavelier, and L. Pagani (eds)

WEAK LENSING SURVEY OF GALAXY CLUSTERS IN THE CFHTLS DEEP FIELDS

G. Soucail[1] and R. Gavazzi[1]

Abstract. The present work proposes to carry out weak lensing mass reconstructions in the CFHTLS Deep fields and focus on high convergence peaks in order to shed light on WLCS capabilities. Among the 14 peaks found above a signal-to-noise detection threshold n=3.5, eight are secure detections with estimated redshift $0.15 < z < 0.6$ and a velocity dispersion $450 < \sigma_v < 600$ km/s.

1 Introduction

With the advent of wide field imaging surveys, the idea of a direct weak lensing cluster survey (hereafter WLCS), aimed at building a mass-selected cluster sample becomes feasible. Building a true mass-selected sample may have strong cosmological implacations as it is directly comparable to CDM theory (through N-body cosmological simulations). The present work proposes to carry out weak lensing mass reconstructions in the CFHTLS-Deep fields and focusses on high convergence peaks in order to shed light on WLCS capabilities.

All the details of this work can be found in Gavazzi & Soucail (2006). Here we present a subset of the main work and focus on the cluster identification.

2 The data set and the weak lensing analysis

For the weak lensing analysis, we used the T0002 release of the CFHTLS-Deep. 4 independant fields of 1 deg^2 each are observed in 5 bands (D1, D2, D3, D4). About 20% of the total area is masked by bright stars, fields boundaries, defects in the CCDs and gaps between them, resulting in a total area of analysis of 3.6 deg^2. For homogeneity background sources are selected with the same criteria in the 4 fields: $22 < i' < 26$.

In order to measure accurately the shape and ellipticities of the background sources, we first correct for the blurring and distorsion introduced by instrument defects, optical aberration, telescope guiding and atmospheric effects. The mapping of the PSF is built from measures of the shape parameters of the stars spread over the whole field. The PSF spatial variation across the field is fitted by a second order polynomial, applied individually to each one of the 36 CCDs composing the MegaCam focal plane. The PSF anisotropies correction is then applied, using the so-called KSB method (Kaiser et al. 1995). From the locally averaged source ellipticities converted into a shear field, we build the convergence maps by integrating the signal over the whole field.

For the detection of significant mass peaks, we estimate the noise level of the reconstructed mass maps which depends directly to the density of backgroupnd sources $n_{\rm bg}$, the size of the smoothing kernel θ_s and the intrinsic variance of the source ellipticities σ_e. Mass maps are then built in units of the signal-to-noise ratio (SNR or ν): $\nu = {\rm SNR} = \kappa\ (4\pi n_{\rm bg}\theta_s^2)^{1/2}/\sigma_e$

In the present data we detect 46 positive peaks with $\nu > 3$ and 5 peaks with $\nu > 4$. In order to avoid too much contamination by noise peaks but to detect as much true peaks as possible, we therefore fix the detection threshold of our cluster sample at $\nu = 3.5$. The 14 peaks detected within this limit constitute the working sample of the CFHTLS-Deep. For a direct estimate the lens redshift of the detected peaks, we implement the lens tomography method proposed by Hennawi and Spergel (2005), using the photometric redshift of the sources. The basics of the method is the following: in the case of a real deflector at redshift z_L, the shear signal must increase in a characteristic way as a function of the source redshift according to the D_{LS}/D_{OS} term. The shape of the shear increase versus the source redshift allows to derive a lens redshift estimate, which is provided for each of the detected peaks.

[1] Observatoire Midi-Pyrénés, 14 Avenue Belin, 31400 Toulouse, France

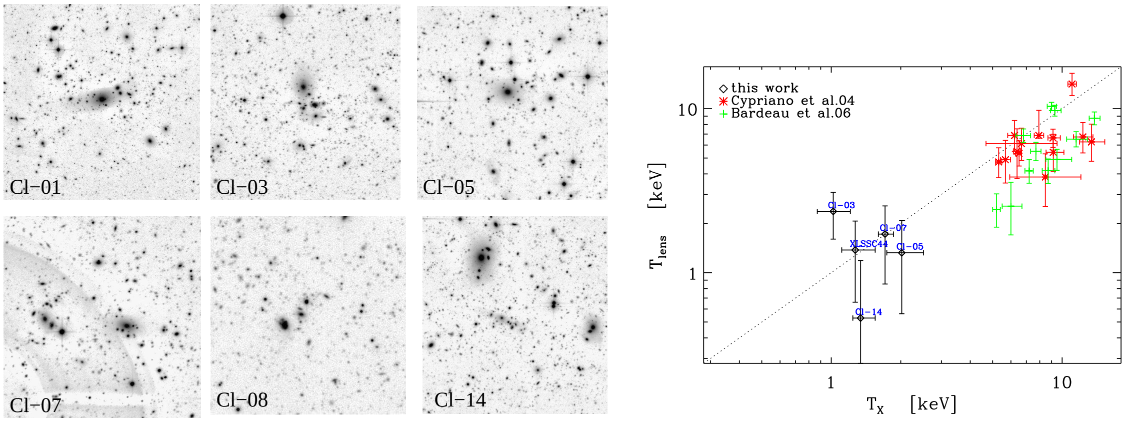

Fig. 1. Left: Cluster optical identification of 6 of the most significant peaks in terms of S/N in the lensing mass reconstruction. Right: Comparison between the cluster temperature inferred from the weak lensing mass and the X-ray temperature, for the clusters cross-identified with the XMM-LSS clusters.

3 Clusters and their X-rays counter-parts

The CFHTLS-Deep D1 field is part of the XMM-LSS. We therefore took advantage of the publicly available X-ray database to cross-correlate our sample of clusters with those X-ray detections already published. The matching is very good: over the seven $\nu > 3.5$ peaks, four are XMM-LSS clusters with luminosity $1.5\,10^{43} < L_{\rm X,bol} < 6.5\,10^{43}$erg/s and temperature $1 < T_X < 2$ keV. Another one is detected at $\nu = 3.4$ (just below our detection limit) and is added in the analysis. The lensing velocity dispersion (inferred temperature $kT_{\rm lens} = \mu m_H \sigma_v^2$ of dark matter particles) and the X-ray temperature are compared for these five clusters (Fig. 1). We include in the comparison data from other weak lensing studies (Cypriano et al. 2004, Bardeau et al. 2007) of X-ray bright clusters. Under the assumption of energy equipartition these temperatures would be equal. If non gravitational sources of gas heating/cooling are at work we expect some departures from this relation. Conversely the mass of shear-selected clusters may be increased by projections of unrelated material along the line of sight. Despite a low numbers statistics the results suggest that shear-selected clusters are well aligned onto the bisectrix while this behaviour seems to be less true for massive clusters. This supports the presence of off-equilibrium physical processes (unrelaxed clusters, merging) as efficient sources of gas heating by shocks.

4 Future prospects

Our cluster candidates are not very massive systems but look more like small clusters / large groups having $400 < \sigma_v < 600{\rm kms}^{-1}$. Most of them lie at redshift ~ 0.3 and all the D1 XMM-LSS clusters that lie in the lensing relevant redshift range $0.1 < z < 0.6$ are detected with a SNR $\nu > 3.4$. The completeness of WLCSs is however lower than X-ray techniques for clusters detections. In addition, the relatively high sample variance of the Deep images prevents any cosmological application of WLCSs but the great depth and amount of photometry make us with an excellent laboratory for a future application to the Wide data. Both WLCSs (with cluster identifications) and raw κ-peaks statistics are complementary applications of weak gravitational lensing. They can provide new insightful constraints on the evolution of large-scale structure driven by Dark Matter and on the behaviour of Dark Energy as a function of redshift.

References

Bardeau, S., Soucail, G., Kneib, J. P., et al. 2007, submitted

Cypriano, E. S., Sodré, L. J., Kneib, J.-P., & Campusano, L. E. 2004, ApJ, 613, 95

Gavazzi, R. & Soucail. G., 2007, A&A in press, astro-ph/0605591

Hennawi, J. F. & Spergel, D. N. 2005, ApJ, 624, 59

Kaiser, N., Squires, G., & Broadhurst, T. 1995, ApJ, 449, 460